Mechanisms of reactions conducted on α-amido-α-aminonitrones, determined based on the structures of their crystalline products and DFT calculations†

Bartosz Trzewik,*[a] Tomasz Seidler,[a] Ewa Brocławik[b] and Katarzyna Stadnicka[a]

Received (in Montpellier, France) 12th March 2010, Accepted 4th May 2010
DOI: 10.1039/c0nj00193g

The crystal structures of several compounds obtained from recently synthesised α-amido-α-aminonitrones were determined by X-ray diffraction. The compounds belonged to three different classes: 1,2,5-oxadiazin-4-ones, amidines and dibenzo[*d*,*f*][1,3]diazepines. In spite of the fact that they were yielded in reactions of various kinds, all the products contained the same amido-amidine moiety. We discovered that some geometrical parameters within the moiety had non-typical values; for example the C_{sp^2}–C_{sp^2} single bonds were outstandingly long. A detailed analysis of the products' geometry, aided by DFT calculations for selected structures, allowed us to propose mechanisms of their formation.

Introduction

Although the determining of crystal structures is a widely used method in the elucidation of enzymatic reaction paths, there have only been a few examples confirming the mechanisms of typical organic reactions, either in the solid state or in solution, by this means. Usually, the structures of crystalline products are determined in order to cast light on reaction mechanisms.

In some cases, however, crystal structures have been found for both the substrates and products of the reactions conveyed, respectively: only in solution,[1] in the solid state and in solution,[2] and exclusively in the solid state.[3] In the case of cyclotriphosphazene hexachloro derivatives,[1] the structural data for the substrate and products of subsequent nucleophilic substitutions by *t*-BuNH groups gave rise to conclusions about the fine detail of the mechanism and revealed the reasons for the suppression of hexasubstitution. Extensive studies by Fu *et al.*[2] upon the versatile reactivity of 9,10-dihydro-9,10-ethenoanthracene derivatives allowed a distinction to be made between different photolytic reaction paths in the solid state and in solution. Furukawa and Matsumoto[3a] succeeded in observing a structural change in a single crystal during the photopolymerisation of muconates diastereomers. Last but not least, Hosoya *et al.*[3b] observed the topochemical photoisomerisation of *N*,*N*-dibenzyl-1-cyclohexenecarbothioamide to an optically active β-thiolactam and were able to determine—using neutron diffraction—the mechanism of hydrogen transfer and prove its intramolecular nature after isotope labelling.

As can be seen in the above examples, X-ray or neutron diffraction can serve as a powerful tool for confirming proposed reaction mechanisms, even in cases where the reactions are performed in solution. It should also be kept in mind that spectroscopic methods routinely used for investigating organic reaction products and reaction mechanisms do not always provide full and unequivocal information about the three-dimensional molecular structures of the products.

In this paper, the results of X-ray diffraction measurements, performed for crystals of novel α-amido-α-aminonitrones and various products of their transformations, allowed us to propose the mechanisms of these reactions. The crystallographic data were combined with appropriate DFT calculations concerning the molecular and electronic structures of the substrate, the products of reactions under dialkylation conditions and the postulated deprotonated intermediate in order to support the selected steps of the proposed mechanisms.

Results and discussion

Crystal structures of the products

During the research upon using novel α-amido-α-aminonitrones, such as **5a**,[4] for constructing heterocyclic systems, several new compounds, shown in Scheme 1, were synthesised.[5] The compounds discussed in this paper belong to three different classes: 1,2,5-oxadiazin-4-ones (**6a,b**), amidines (**7a,b**) and dibenzo[*d*,*f*][1,3]diazepines (**11a,b**). Crystal structures of four of them—**6b**, **7a**, **7b** and **11a**—are described here for the first time. Crystal data, experimental conditions and details of refinement procedures are given in Table 1.

The results of the X-ray crystal structure analysis performed for the products of the reactions provided unequivocal information about the molecular structures of **6**, **7** and **11**.

In reactions with aromatic biphenyl-2,2′-diamine, seven-membered rings of dibenzo[*d*,*f*][1,3]diazepines **11** were formed as the result of disubstitution on the carbon atom adjacent to

[a] *Faculty of Chemistry, Jagiellonian University, ul. Romana Ingardena 3, 30-060 Kraków, Poland. E-mail: trzewik@chemia.uj.edu.pl; Fax: +48 12 634 05 15; Tel: +48 12 663 22 97*
[b] *Institute of Catalysis and Surface Chemistry PAN, ul. Niezapominajek 8, 30-239 Kraków, Poland. E-mail: broclawi@chemia.uj.edu.pl; Tel: +48 12 663 20 23*

† CCDC reference numbers: 750328–750331. Electronic supplementary information (ESI) available: (1) geometric parameters of weak interactions in the crystalline state; (2) packings of molecules **6b**, **7a**, **7b** and **11a**. For ESI and crystallographic data in CIF or other electronic format see DOI: 10.1039/c0nj00193g

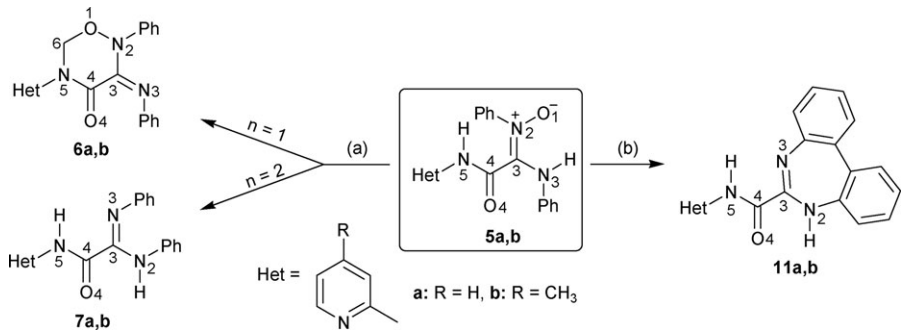

Scheme 1 Chemical structural formulae of the products obtained from nitrones **5a,b**.[5] Reagents and conditions: (a) $(CH_2)_nI_2$, NaH (2 equiv.), anhyd DMF, −10 °C to r.t., 1.5 h; (b) biphenyl-2,2′-diamine, TsOH (cat.), AcCN, reflux, 2 h. Compound **7a** is reported here for the first time.

Table 1 Crystal data, experimental conditions and details of refinement procedures

	6b	**7a**	**7b**	**11a**
Chemical formula	$C_{21}H_{18}N_4O_2$	$C_{19}H_{16}N_4O$	$C_{20}H_{18}N_4O$	$C_{19}H_{14}N_4O$
M/g mol^{-1}	358.39	316.36	330.38	314.34
Crystal system, space group	Triclinic, *P*-1	Monoclinic, *C*2/*c*	Monoclinic, $P2_1/c$	Triclinic, *P*-1
T/K	293(2)	293(2)	293(2)	293(2)
a/Å	10.3512(3)	26.1851(8)	13.5564(3)	10.3641(2)
b/Å	10.5145(3)	9.1055(3)	10.1570(3)	11.7961(3)
c/Å	10.8469(4)	13.7491(6)	13.3227(4)	14.4961(4)
α (°)	116.607(2)	90.000	90.000	89.766(1)
β (°)	115.147(2)	98.881(1)	109.473(1)	69.834(1)
γ (°)	94.549(2)	90.000	90.000	70.166(1)
V/Å^3	900.91(6)	3238.9(2)	1729.50(8)	1552.07(7)
Z (Z')	2	8	4	4 (2)
D_x/Mg m^{-3}	1.321	1.298	1.269	1.345
μ/mm^{-1} (Mo-K$_\alpha$)	0.09	0.08	0.08	0.09
Crystal colour	Yellow	Yellow	Yellow	Orange
Crystal size/mm	0.60 × 0.38 × 0.25	0.57 × 0.32 × 0.05	0.60 × 0.57 × 0.03	0.30 × 0.12 × 0.07
Absorption correction[a]	Multi-scan	Multi-scan	Multi-scan	Multi-scan
T_{min}, T_{max}	0.949, 0.978	0.954, 0.996	0.953, 0.998	0.973, 0.994
Reflections collected[b], unique, observed [$F^2 > 2\sigma(F^2)$]	5519, 4077, 3031	5189, 3630, 2814	6633, 3945, 2532	9212, 6016, 3947
R_{int}	0.026	0.022	0.030	0.033
θ_{max} (°)	27.5	27.5	27.5	26.0
R_1 [$F^2 > 2\sigma(F^2)$], wR_2 (all F^2), S	0.048, 0.135, 1.00	0.045, 0.115, 1.04	0.054, 0.125, 0.99	0.061, 0.129, 1.05
Reflections/parameters	4077/244	3630/223	3945/233	6016/445
Weighting scheme[c] a, b	0.0609, 0.2162	0.0407, 1.7843	0.0442, 0.5708	0.0402, 0.4713
$(\Delta/\sigma)_{max}$	<0.001	0.001	<0.001	<0.001
$\Delta\rho_{max}$, $\Delta\rho_{min}$/e Å^{-3}	0.18, −0.18	0.17, −0.17	0.14, −0.15	0.19, −0.20

[a] HKL DENZO and Scalepack.[6a b] COLLECT.[6b c] Weighting scheme: $w = 1/[\sigma^2(F_o^2) + (aP)^2 + bP]$ where $P = [\max(F_o^2, 0) + 2F_c^2]/3$.

the nitrone moiety (Scheme 1). The results of the reactions of **5** with dialkylation agents turned to be more stimulating: compounds **6** and **7**, though chemically different, were formed under similar conditions. The only difference was in the number of methylene groups between the iodine atoms in the dialkylation agent molecules (Scheme 1). On the other hand, there was a pronounced similarity of the chemical structures of amidines **7** and compounds **11**, in spite of the fact that they were formed in totally different processes. Molecules of **11** differed from those of **7** in the presence of a single bond between the phenyl rings (for the overall shapes of the molecules under discussion, see Fig. 1). This made **7** and **11** interesting for a comparison from a crystallographic point of view. The most salient details of the geometrical parameters of the molecular core, which is the same in all the products, are given in Table 2.

Surprisingly, the dihedral angles between the phenyl rings in the molecules of **7** and **11** were not influenced by the presence of the C26–C36 single bonds in the molecules of **11**. However, significant differences in the values of the C21–N2–C3–N3 torsion angles were observed.

The $C3_{sp^2}$–$C4_{sp^2}$ single bonds in the molecules of all the studied compounds were particularly long (in the range between 1.517 Å in **11a** and 1.536 Å in **6a**). We attribute this phenomenon to the electron withdrawing effect of the substituents at both ends of the bonds (N2 and N3 atoms at C3, and O4 and N5 atoms at C4). Concerning the oxadiazine rings of **6a,b**, the effect was enhanced by strain in the six-membered rings, caused by the relatively short C4–N5, C3–N2 and N2–O1 single bonds (see Table 2). In the molecules of **7a,b** and **11a,b**, the elongation of the $C3_{sp^2}$–$C4_{sp^2}$ single bonds could additionally be attributed to the effect of short intramolecular separations of the N2–H2···O4 and N5–H5···N3 type. These "short intramolecular separations" can be considered "hydrogen-bond-like interactions"[9a] (see Table 3), closing five-membered quasi-rings. This conclusion is based

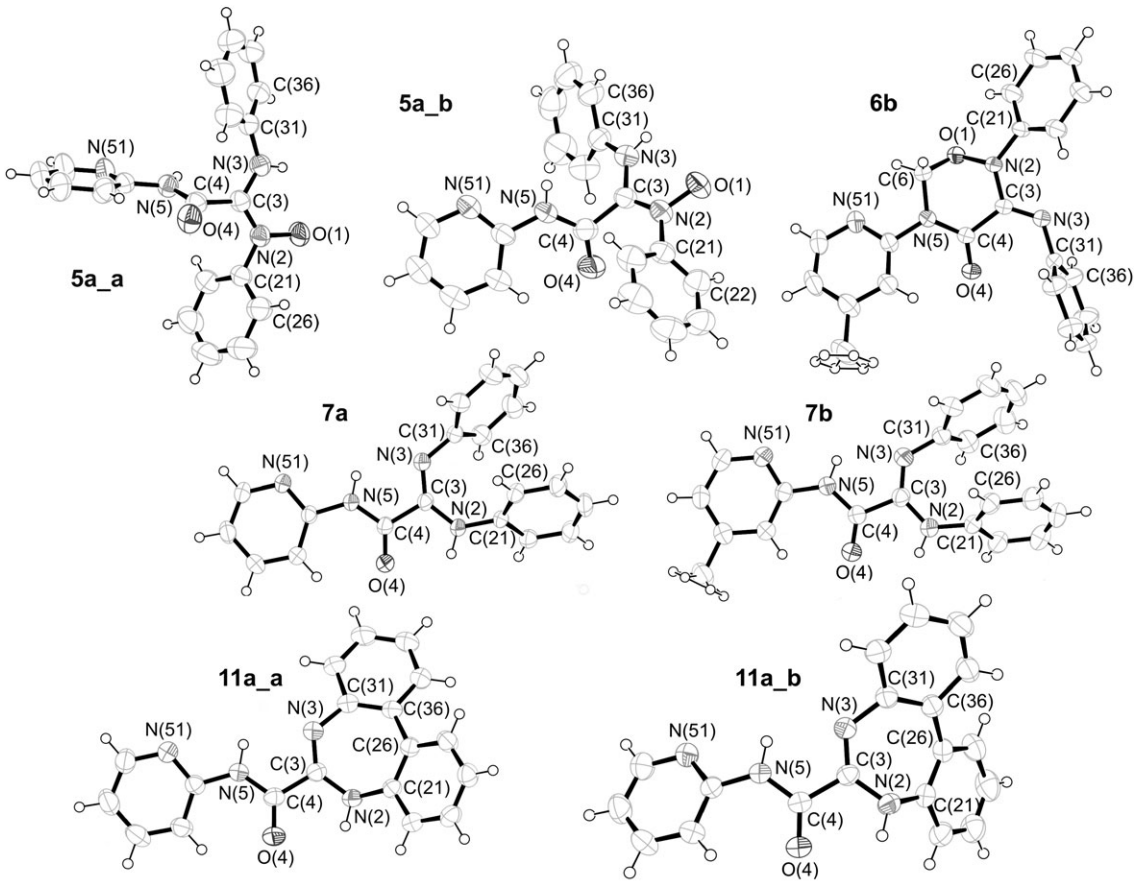

Fig. 1 The overall shapes of the molecules under discussion, in comparison to substrate molecules **5a_a** and **5a_b**, presented as ORTEP3[7] projections onto the core N-atoms (N2, N3 and N5). Displacement ellipsoids of non-hydrogen atoms are drawn at the 50% probability level. The numbering schemes are given only for significant atoms. Molecules **11a_a** and **11a_b** both have two chirality axes, and in crystal structure they constitute pairs of conformational diastereomers.

Table 2 Comparison of selected geometrical parameters (distances Å and angles °) for the molecular core[a] of the compounds from this work: **6b**, **7a**, **7b** and **11a**, and of those previously published: **5a**,[4] **6a**[5] and **11b**[8]

	5a_a	5a_b	6a	6b	7a	7b	11a_a	11a_b	11b
N2–C3	1.347(3)	1.342(3)	1.387(2)	1.386(2)	1.356(2)	1.351(2)	1.370(3)	1.375(3)	1.364(1)
C3–N3	1.315(3)	1.311(3)	1.263(2)	1.264(2)	1.286(2)	1.285(2)	1.275(3)	1.279(3)	1.278(1)
C3–C4	1.511(3)	1.516(4)	1.536(2)	1.535(2)	1.526(2)	1.525(2)	1.517(3)	1.517(3)	1.524(1)
C4–N5	1.343(3)	1.343(3)	1.369(2)	1.368(2)	1.349(2)	1.349(2)	1.347(3)	1.352(3)	1.335(1)
N2–O1	1.336(2)	1.344(2)	1.416(2)	1.420(2)					
N2–C3–C4	122.5(2)	123.0(2)	114.2(1)	114.0(1)	110.5(1)	110.6(2)	113.1(2)	114.9(2)	112.7(1)
N2–C3–N3	117.8(2)	118.2(2)	120.9(1)	120.4(1)	133.2(1)	132.9(2)	130.2(2)	128.7(2)	130.1(1)
O4–C4–N5	126.0(2)	126.9(2)	124.6(2)	124.2(1)	125.2(1)	125.2(2)	125.3(2)	125.0(2)	126.0(1)
C3–C4–N5	114.3(2)	113.8(2)	116.1(1)	116.2(1)	114.0(1)	113.9(2)	113.5(2)	113.9(2)	113.7(1)
C21–N2–C3–C4	13.9(3)	−10.3(4)	179.9(2)	−178.1(1)	−171.2(1)	−174.1(2)	143.1(2)	130.0(2)	139.6(1)
N3–C3–C4–O4	61.7(3)	−57.1(3)	−14.9(2)	−17.0(2)	177.9(1)	177.0(2)	−175.0(2)	179.1(2)	178.5(1)
N2–C3–C4–O4	−115.0(3)	121.4(3)	170.0(2)	168.9(2)	−1.6(2)	−2.7(3)	8.3(3)	−0.7(3)	−4.9(2)
N2–C3–C4–N5	−118.6(2)	123.6(2)	−13.0(2)	−13.5(2)	179.7(1)	178,5(2)	−171.1(2)	−179.1(2)	173.7(1)
N3–C3–C4–N5	64.7(3)	−57.8(3)	162.1(2)	160.6(2)	−0.8(2)	−1.7(2)	5.7(3)	0.6(3)	−2.8(2)
C21–N2–C3–N3	−169.2(2)	171.1(2)	4.6(3)	7.5(2)	9.4(3)	6.1(4)	40.7(3)	−49.7(3)	−44.4(2)
N2–C3–N3–C31	−166.1(2)	159.7(2)	168.9(2)	171.6(1)	8.2(3)	6.8(3)	9.8(3)	−6.8(4)	4.9(2)
C31–C36–C26–C25							−148.5(2)	149.0(2)	148.6(1)
C35–C36–C26–C25							30.2(3)	−29.1(3)	−29.8(2)
C31–C36–C26–C21							33.9(3)	−35.2(3)	−34.2(2)
C35–C36–C26–C21							−147.4(2)	146.7(2)	147.5(1)
∠core[a], C21^C26			37.21(6)	46.79(8)	46.99(5)	56.40(6)	34.23(8)	45.76(8)	37.71(5)
∠core[a], C31^C36			76.69(6)	78.46(5)	55.46(6)	58.21(7)	25.62(12)	31.62(8)	26.51(5)
∠C21^C26, C31^C36			82.31(7)	75.78(7)	33.39(6)	23.39(7)	32.17(11)	32.56(12)	32.01(6)

[a] The best plane defined by atoms of the amido-amidine moiety, identical for all the compounds: N2, C3, N3, C4, O4, N5.

Table 3 Geometry of intermolecular hydrogen bonds and hydrogen-bond-like intramolecular interactions (marked with asterisks)

D–H···A	D–H/Å	H···A/Å	D···A/Å	D–H···A/°
7a				
N2–H2···O4*	0.89(1)	2.16(2)	2.633(2)	112(1)
N2–H2···N51^{i}	0.89(1)	2.27(1)	3.089(2)	154(1)
N5–H5···N3*	0.87(1)	2.19(2)	2.645(2)	112(1)
7b				
N2–H2···O4*	0.88(1)	2.18(2)	2.634(2)	111(2)
N2–H2···N51^{i}	0.88(1)	2.21(2)	3.026(2)	155(2)
N5–H5···N3*	0.88(1)	2.17(2)	2.646(2)	113(1)
11a				
N2a–H2a···O4a*	0.89(1)	2.24(2)	2.699(2)	112(2)
N5a–H5a···N3a*	0.89(1)	2.20(2)	2.631(3)	110(2)
N2a–H2a···N51b	0.89(1)	2.40(1)	3.248(3)	160(2)
N5a–H5a···O4b^{i}	0.89(1)	2.45(2)	3.151(2)	137(2)
N2b–H2b···N51a^{ii}	0.89(1)	2.17(1)	3.023(3)	159(2)
N2b–H2b···O4b*	0.89(1)	2.30(2)	2.734(2)	110(2)
N5b–H5b···N3b*	0.89(1)	2.18(2)	2.634(3)	111(2)
N5b–H5b···O4a	0.89(1)	2.25(2)	3.000(2)	143(2)
11b				
N2–H2···O4*	0.88(1)	2.22(1)	2.677(1)	112(1)
N5–H5···N3*	0.87(1)	2.19(1)	2.644(1)	112(1)
N2–H2···O4^{i}	0.88(1)	2.31(1)	3.108(1)	151(1)

Symmetry codes for **7a**: (i) $x, -y, z + \frac{1}{2}$; for **7b**: (i) $x, -y + \frac{1}{2}, z - \frac{1}{2}$; for **11a**: (i) $x + 1, y, z$; (ii) $x - 1, y, z$; for **11b**: (i) $-x, -y + 1, -z + 1$.

on solid state and solution state evidence. Other electronic factors supposedly influencing the length of the C3–C4 bonds will be discussed in detail in the next section.

While discussing the X-ray diffraction data, it is worth noting that there are no examples of single C_{sp^2}–C_{sp^2} bonds with the chemical neighbourhood –(O═C)–(C═N)– in the ITC.[9b]

Although there are many examples of structures containing molecules with the –(O═C)–(C═N)– core in the CSD (2008),[9c] only six of them have the extended –N(–H)–C(═O)–C(═N–)–N(–H)– core that is characteristic of the molecules under discussion. Two of them, with refcodes LIVZEW and PILPAC, are **5a** and **11b**. From the remaining four examples (DADHAR, FOWPOW, ICOLAO and PAPKEW), only in one of them (FOWPOW)[9d] is the discussed C_{sp^2}–C_{sp^2} distance greater than 1.500 Å.

The six-membered rings of **6** adopted boat conformations with pseudo-mirror planes (C_s) through the O1, C4 and O4 atoms. The seven-membered rings of **11** adopted twist-boat conformations with pseudo-mirror planes (C_s) through the N3 atoms and the centres of the C21–C26 bonds in each molecule.

The values of the C21–N2–C3 angles were particularly high [129.0(6)° on average] in the cases of the oxadiazine rings of **6**, due to the previously mentioned ring strain. In the cases of **7**, it was probably due to the resonance effect within the N3═C3–N2 fragment. Whereas in the cases of **11**, both of these effects are lacking and the values of the angles are typical [122(1)° on average]. Other high values of valence angles were those of N2–C3–N3 [131(2)° on average]: in **7**—due to intramolecular hydrogen-bond-like interactions (Table 3); in **11**—interactions of this type additionally modified the strain in the non-planar seven-membered rings.

The N3–C3–C4–O4 angles were nearly *s-cis* [−16(1)° on average] in the molecules of **6**, and almost ideally *s-trans* [180(3)° on average] in the molecules of **7** and **11**. The *s-trans* conformations were preserved due to intramolecular hydrogen-bond-like interactions of the N–H···O and N–H···N type, the effect of which was clearly pronounced.

The presence of such interactions, even in solution ($CDCl_3$), could be also related to downfield shifts of the H-atom signals for CONH and NH groups visible in ^{1}H NMR spectra; the signals were recorded, respectively, at 10.54 and 8.42 ppm for **7b**, and 10.25–10.21 and 7.62–7.61 ppm for **11a,b**.[5]

A further premise for the existence of hydrogen-bond-like intramolecular interactions of the N–H···O═C type in molecules **7b**, **11a** and **11b** were the $\nu_{C=O}$ values in the IR spectra acquired in KBr (*i.e.* in the solid state). They were equal to 1702, 1687 and 1694 cm^{-1} for **7b**, **11a** and **11b**, respectively. These values are remarkably high for amide C═O bonds.

Compound **11a** crystallised with two symmetry-independent conformational diastereomers in the asymmetric unit, **11a_a** and **11a_b**. This conformational diastereoisomerism arose from the presence of two chirality axes: one of them is defined by the C26–C36 biphenyl single bond, the other embraces the C3–C4 single bond (the single C3–C4 bond links the two distinct parts of the molecules: the amide part, including the pyridine ring, and the benzodiazepine moiety).

Considering a molecule with a chirality axis, one has to determine the configuration around the axis according to Cahn–Ingold–Prelog rules (see Fig. 2). It should be stressed that the configuration is irrespective of the view direction. In the cases of molecules **11a_a**, **11a_b** and **11b**, the configurations around the chirality axes, embracing the C3–C4 bonds, can be related to the signs of the ②–C3–C4–③ (Fig. 2a) or ②–C4–C3–③ (Fig. 2b) torsion angles. Their signs are positive in the cases of *R* configurations, otherwise they are negative (see the signs of angles N2–C3–C4–O4 and N3–C3–C4–N5 in Table 2 for comparison). These relations depend on the relative priorities of the substituents in each studied case.

In respect to the C3–C4 axis, **11a_a** has with no doubt an *R* configuration [N2–C3–C4–O4 = 8.3(3)° or N3–C3–C4–N5 = 5.7(3)°]. In molecule **11a_b**, the picture is more complex as the respective angles are very close to 0° and have opposite signs [N2–C3–C4–O4 = −0.7(3)° or N3–C3–C4–N5 = 0.6(3)°] (Fig. 2c and d). This made us unable to differentiate between the *S* and *R* configuration. Looking from the C4 end of the axis towards C3, the determined configuration would be *S*, while looking from the C3 end of the axis towards C4 one would determine an *R* configuration (Fig. 2). However, as was mentioned earlier, the absolute configuration should be independent from the direction of observation.

Regarding the C26–C36 single bond, the absolute configuration of **11a_a** could be designated as *S* [C31–C36–C26–C21 = 33.9(3)° or C35–C36–C26–C25 = 30.2(3)°] and that of **11a_b** as *R* [C31–C36–C26–C21 = −35.2(3)° or C35–C36–C26–C25 = −29.1(3)°].

Discussing the molecular geometry of molecules **11a_a** and **11a_b**, one should keep in mind that the crystal structure is racemic (space group *P*-1). The structure of **11b** is simpler: in the asymmetric unit, it had one molecule with an *R* configuration on the biphenyl C26–C36 single bond [C31–C36–C26–C21 = −34.2(2)° or C35–C36–C26–C25 = −29.8(2)°] and an *S* configuration on the C3–C4 single bond

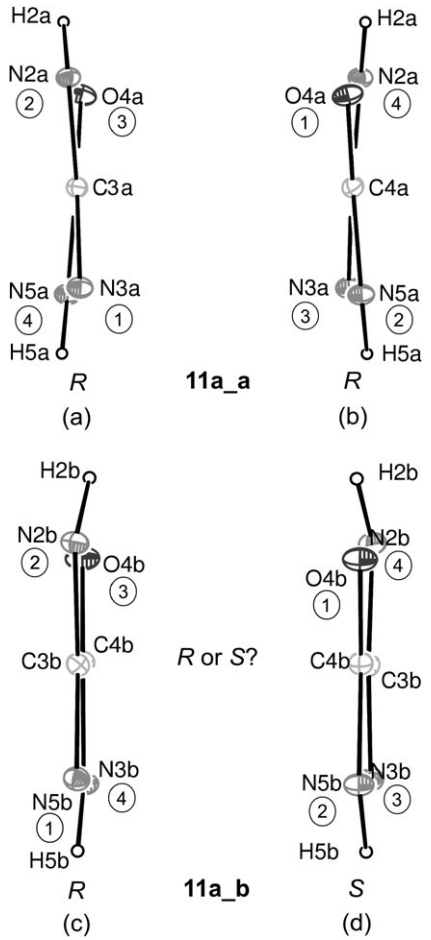

Fig. 2 The amido-amidine cores of molecules **11a_a** and **11a_b** in ORTEP3[7] projections approximately along their C3–C4 chirality axes. The cores on the left are seen from the C3 ends of the axes; the cores on the right are seen from the C4 ends. In each projection, numbers in circles denote the priority of substituents around the axis according to Cahn–Ingold–Prelog rules. The substituents closer to the observer are of higher priority, the other rules remain the same as in the case of a C_{abcd} chirality centre. The absolute configurations around the chirality axes were determined in each case and are given under each projection.

[N2–C3–C4–O4 = −4.9(2)° or N3–C3–C4–N5 = −2.8(2)°], and, obviously, its centrosymmetric image was present in the structure (space group *P*-1).[8]

Geometrical details of the intermolecular hydrogen bonds and hydrogen-bond-like intramolecular interactions of N–H···O and N–H···N type in molecules **7a**, **7b**, **11a** and **11b**[8] are given in Table 3.

Moving to the products of the reactions under dialkylation conditions—**7** and **11**—the N2–H2···O4 and N5–H5···N3 intramolecular hydrogen-bond-like interactions stabilised the molecular conformations by forming five-membered quasi-rings so that the double bonds C4═O4 and C3═N3 were in *s-trans* positions [the mean value of N3–C3–C4–O4 = 180(3)°].

All the above values of geometrical parameters given for **6a** were confirmed by DFT calculations, performed for single molecules both in a vacuum and in a DMF environment (Table 4).

Proposed reaction mechanisms and DFT calculations

The versatile reactivity of nitrones **5** against various dialkylation reagents encouraged us to propose mechanisms for these reactions. The mechanisms, based on the results of the X-ray structure analyses and DFT calculations, are depicted in Scheme 2 and will be discussed in detail, along with the results of the calculations.

We did not attempt to model full reaction pathways since the crucial steps would have required an explicit inclusion of alkyl diiodides, which would have made the calculation of critical structures very cumbersome (because of the heavy iodine atoms and the almost free rotation of CH_2 groups).

The geometry of starting nitrones **5** (for example **5a**) were determined both experimentally in the crystalline state and *in silico* for single molecules in a vacuum and in a reaction medium (DMF). The obtained results are compared in Table 4.

The core part of molecule of **5a** (Fig. 1) is stabilised by an intramolecular N3–H3···O1 hydrogen bond.

Analysis of the bond lengths, and calculations of NBO[10a] and Merz–Singh–Kolman (MK)[10b,c] atomic populations (Table 5), prompted us to conclude that only mesomeric structures with a meaningful negative charge on the O1 atom gave a significant contribution to the structure of nitrones **5**. This means that, in contrast to (*Z*)-*N*-[(phenylamino)methylene]-aniline oxide,[11] only one tautomeric (nitrone) form prevails in the cases of **5**. As can be seen from Fig. 1 on example compound **5a**, nitrones of type **5** have a *Z* configuration about the C3═N2 double bond. The values of the torsion angles O4═C4–C3═N2 in the core moiety of **5a_a** and **5a_b** were very close to ±60°. This allowed us to describe the mutual arrangement of the double bonds as *gauche*.

As we mentioned in the previous section, we noticed key differences between the conformations of starting nitrones **5** and the resulting 1,2,5-oxadiazin-4-ones **6**, amidines **7** and dibenzo[1,3][*d*,*f*]diazepines **11** (Table 2).

We will now discuss the influence of steric and electronic factors that allowed us obtaining from **5**—under similar conditions—quite different systems, **6** and **7** (Scheme 1).

Let us recall that both **6** and **7** were isolated after reactions under dialkylation conditions with the use of methylene diiodide (one carbon atom) and ethylene diiodide (a two carbon chain), respectively. The reactions required the addition of a two-fold molar amount of NaH to complete. The first step was a deprotonation of the amine N3 atom by the first mole of NaH—the addition of which seemed to be crucial (without NaH, no reaction was observed)—leading to anion **5′**. Concerning substrate molecules **5** (Fig. 1), the existence of the intramolecular N3–H3···O1 hydrogen bond apparently diminished the reactivity of the nitrones in dialkylation reactions, leading to products **6** and **7**. The hydrogen-bond needed to be weakened (if not broken) by an appropriate solvent of high polarity to make the reactions possible. Deprotonation was then facilitated in a highly polar solvent (DMF, ε = 38.2). It should be noted that in less polar solvents, such as THF (ε = 7.5) or toluene (ε = 2.4), the reactions failed. The above observations were strongly supported by the results of DFT calculations in solution: both the lengthening of the H3···O1

Table 4 Selected geometrical parameters (distances Å and angles °) of molecules of **5a** and **6a** calculated *in vacuo* and in a DMF reaction medium, and of a molecule of deprotonated tentative intermediate form **5′a** in DMF, compared with those obtained by X-ray diffraction for **5a** and **6a**

	5a_a (X-ray)	**5a_b** (X-ray)	**5a** (DFT *in vacuo*)	**5a** (DFT in DMF)	**5′a** (DFT in DMF)	**6a** (X-ray)	**6a** (DFT *in vacuo*)	**6a** (DFT in DMF)
N2–C3	1.347(3)	1.342(3)	1.374	1.324	1.349	1.387(2)	1.398	1.387
C3–N3	1.315(3)	1.311(3)	1.327	1.361	1.323	1.263(2)	1.273	1.278
C3–C4	1.511(3)	1.516(4)	1.500	1.509	1.526	1.536(2)	1.541	1.541
C4–N5	1.343(3)	1.343(3)	1.374	1.364	1.369	1.369(2)	1.387	1.376
N2–O1	1.336(2)	1.344(2)	1.302	1.320	1.346	1.416(2)	1.418	1.414
N2–C3–C4	122.5(2)	123.0(2)	122.2	120.9	116.6	113.1(2)	114.7	115.0
N2–C3–N3	117.8(2)	118.2(2)	115.4	116.7	120.5	130.2(2)	120.3	120.3
O4–C4–N5	126.0(2)	126.9(2)	124.9	125.5	124.3	124.6(2)	124.3	124.7
C3–C4–N5	114.3(2)	113.8(2)	112.6	112.8	112.8	116.1(1)	116.5	116.7
C21–N2–C3–N3	−169.2(2)	171.1(2)	166.7	167.0	161.7	4.6(3)	11.9	8.4
N2–C3–N3–C31	−166.1(2)	159.7(2)	140.4	150.8	157.9	168.9(2)	166.6	165.4
C3–N3–C31–C36	−147.9(2)	152.2(2)	166.2	163.9	146.4	−77.8(2)	124.6	126.0
C3–N3–C31–C32	35.0(4)	−32.0(3)	−14.4	−17.3	−38.6	107.9(2)	−63.0	−61.4
C21–N2–C3–C4	13.9(3)	−10.3(4)	−8.7	−9.0	−18.5	179.9(2)	−10.7	−13.6
N2–C3–C4–O4	61.7(3)	−57.1(3)	−43.1	−51.6	−53.7	170.0(2)	−17.2	−17.3

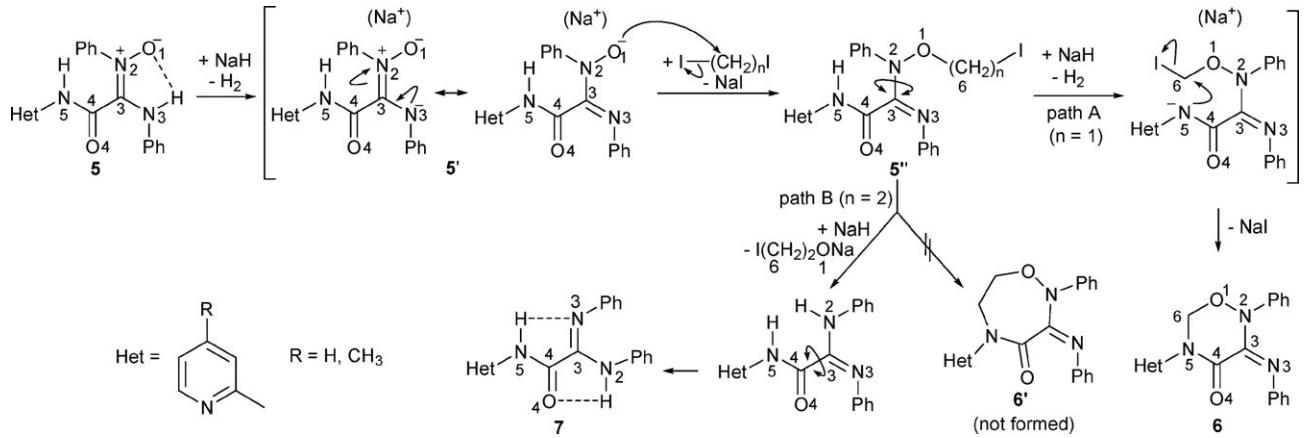

Scheme 2 Proposed mechanisms of forming 1,2,5-oxadiazin-4-ones **6** and amidines **7**.

Table 5 Computed values of selected atomic charges in molecule of **5a** *in vacuo* and in solvents of various polarity

		Atomic charge/*e*			
	Atom	*In vacuo*	In toluene (ε = 2.4)	In THF (ε = 7.5)	In DMF (ε = 38.2)
NBO	N2	0.0170	0.0065	−0.0032	−0.0089
	O1	−0.5656	−0.5985	−0.6267	−0.6418
MK	N2	0.1686	0.1391	0.1208	0.1101
	O1	−0.5080	−0.5520	−0.5921	−0.6149

distance and the lowering of the H3 proton abstraction energy were positively correlated with the increasing solvent polarity (Table 6).

Within the $^{-}$O1–$^{+}$N2=C3–N3 fragment of the deprotonated **5′** molecule, the lone electron pair from the N3 atom formed a new N3=C3 double bond, and the electron pair from the previous C3=N2 double bond counterbalanced the positive charge on the nitrogen N2 atom. The former C3=N2 bond then became a C3–N2 single bond. Such an electron density flow is possible only within a planar moiety providing significant p orbital overlap.

This observation was confirmed by quantum-chemical calculations. The value of the C3=N3 bond length, equal to 1.324 Å in **5a**, increased to 1.349 Å in molecule **5′a**, whereas

Table 6 Relative energies of **5a** before and after the deprotonation and the H3···O1 distance in a molecule of **5a** in various environments

Environment	ΔE (= $E_{\mathbf{5a}} - E_{\mathbf{5'a}}$)/kcal mol^{-1}	Deviation from ΔE *in vacuo*/kcal mol^{-1}	$d_{H3\cdots O1}$/Å	H3···O1 elongation from *d in vacuo*/Å
In vacuo	347		2.032	
Toluene	326	−21	2.050	0.018
THF	310	−37	2.088	0.056
DMF	301	−46	2.104	0.072

Table 7 Bond populations for selected bond natural orbitals in the **5a**, **5′a** and **6** molecules (*in vacuo*)

NBO description	Bond population		
	5a	**5′a**	**6**
π C3–N2	1.924	—	—
π C3–N3	—	1.834	1.842
LP N3	1.716	1.812	1.822
LP O4	1.858	1.864	1.850
σ* C3–C4	0.074	0.091	0.104

the length of the C3–N2 bond, equal to 1.361 Å in molecule **5a**, decreased to 1.323 Å in **5′a** (Table 4). Simple geometrical considerations were also fully paralleled by NBO analysis, as summarized in Table 7.

The double bond between C3 and N2, populated by nearly 2 electrons in **5a**, looses its π component in **5′a** and **6**. On the contrary, the double bond between C3 and N3 showed up only in **5′a** and **6**. An antibonding C3–C4 σ* orbital gained some population that goes in line with bond elongation in the series **5**, **5′a** and **6** (both measured and calculated).

An analysis of the corresponding second order energy contributions indicated, however, that the σ* orbital population was mainly due to the interaction with the O4 lone pair in **5a** (E^2 = 20.48 kcal mol^{-1}), while it was with the N3 lone pair in **5′a** and **6** (E^2 = 12.68 and 13.93 kcal mol^{-1}, respectively).

A somewhat surprisingly low population of the N3 lone pair in **5a** came from its strong interaction with antibonding π* orbitals of the C3═N2 bond and the phenyl ring—this interaction is not critically relevant for geometrical parameters.

In products **7**, the mixing with the N3 lone pair should be ineffective (in analogy to substrates **5**). Therefore, the lengthening of C3–C4 bond in **7a** in comparison to **5a** (1.526 *vs.* 1.511–1.516 Å) should be attributed to the intramolecular hydrogen-bond-like interactions of the N–H···N and N–H···O type. This could also be concluded from the downfield shifts of the signals of the respective H atoms in their ^{1}H NMR spectra, as mentioned earlier.

Anions **5′** remained nearly planar within the discussed moiety, as could be seen from the calculated value of −9.9° for the O1–N2–C3–N3 torsion angle. We postulate that the nitrone oxygen atom O1 is alkylated first, leading to monoalkylated intermediates **5″** (Scheme 2).

The deprotonation of the amide N5 nitrogen atom by the second mole of NaH made the second alkylation possible. In the case of using methyl diiodide (Scheme 2—path A), the ring closure indeed occurred, leading to 1,2,5-oxadiazin-4-ones **6**. A question arose as to why, in the case of using ethylene diiodide, no alkylation took place and the whole reaction was instead a deoxygenation, affording **7** (Scheme 2—path B).

DFT calculations suggest that the dramatic change in the last step of the reaction was not the result of the difference in size of the –CH_2– and –CH_2–CH_2– groups, as one might assume. In the case of using ethylene diiodide, the second alkylation could have formed seven-membered rings of **6′** (see Scheme 2). The calculations revealed that the introduction of an additional –CH_2– group into these putative products **6′** would have not introduced any additional strain. As can be seen for examples **6a** and **6′a**, the computed ΔE is practically equal to E_{CH_2} (Table 8). Apparently, the reason accounting for the reaction running along path B, leading to products **7**, seems to be *not* thermodynamic, but rather kinetic in nature.

Table 8 The differences in energies of molecule **6a** and the molecule of the putative seven-membered compound **6′a**, compared with the energy of a –CH_2–group *in vacuo* and in DMF

Environment	ΔE (= $E_{6'a}$ − E_{6a})/kcal mol^{-1}	ΔE − E_{CH_2}/kcal mol^{-1}
In vacuo	−39.317	0.000
DMF	−39.319	0.002

Path B consists in a reduction of monoalkylated nitrone moiety **5″** by the second mole of NaH. It is known that the N–O nitrone bond is rather weak and is prone to breaking.[12] In the reaction of **5** with methyl diiodide, paths A and B compete to some extent: along with the main products **6**, small amounts of products **7** are also formed.

The double bonds in the molecules of products **7** adopt an *s-trans* conformation, instead of *s-cis* as in **6**. This can be reasoned by the forming of several stabilising interactions; between them, the two of intramolecular hydrogen-bond-like type play the most important role (Table 3). The formation of **11** from **5** and biphenyl-2,2′-diamine is an example of quite a different reactivity of α-amido-α-aminonitrones **5**. The mechanism seems to be simple and unequivocal here: the reaction can be treated as an acid-catalysed bi-nucleophilic attack of the two amine groups of biphenyl-2,2′-diamine on the C3 atom in molecules of nitrones **5**. Formally, this reaction is both a transamination and an imine formation.

In this case, the nitrone moiety acts as an active equivalent of a carbonyl group.[13] The *s-trans* arrangements of the C═O and C═N bonds in the cores of products **11** is an effect of the two hydrogen-bonding-like stabilisations (analogous to that in **7**), as well as an attempt to minimize steric hindrance between the rigid and bulky benzodiazepine moiety and the amide moiety in molecules **11**.

Conclusions

The results of the X-ray structure analysis of both α-amido-α-aminonitrones and products of their transformations were utilised in three ways.

From a synthetic point of view, the unequivocal determination of the constitution of the reaction products allowed us to show the flexibility and utility of the starting nitrones in organic synthesis.

Regarding the geometrical parameters of the compounds in question, we discovered an outstandingly long, up to 1.536(2) Å, C_{sp^2}–C_{sp^2} single bond. The bond joins the amide and the amidine parts of the molecular core, common to all the compounds: the substrates and the products. It seems that this feature, together with the high value of the N_{sp^3}–C_{sp^2}–N_{sp^2} valence angle, 131(2)° on average in **7** and **11**, are connected with the specific constitution of the core. It is worth noting that the intramolecular hydrogen-bond-like interactions, of N–H···O and N–H···N type, significantly influenced both the geometrical parameters of the cores of product molecules and the mechanisms of their formation.

Most importantly, the detailed structural data analysis cast light on the nature of the studied reactions, especially those leading, under similar conditions, to the different products **6** and **7**.

The DFT calculations performed for isolated molecules of **5a** and **6a** reproduced correctly, and rationalised the unusual length of the C_{sp^2}–C_{sp^2} single bond. On the other hand, the modelling performed for molecules **5a**, **5′a**, **6a** and **6′a** in the reaction medium (DMF) strongly supported the importance of a polar medium in the proposed mechanism for the formation of the oxadiazines **6**, and rationalised the reasons for yielding amidines **7** under similar conditions.

In our opinion, the results presented above point to the possibility of applying combined structural research (X-ray structure determination and DFT calculations) to the elucidation of organic reaction mechanisms, even those carried out in solution.

Experimental

Melting points were determined on an Electrothermal IA9000 digital melting point apparatus (±0.5 °C) and were not corrected. Yields are given for the pure products.

Synthesis[5] and crystal preparation

(*Z*)-2-Anilino-2-[oxido(phenyl)imino]-*N*-pyridin-2-yl-acetamide (5a). (2.70 g, 81%): white powder; mp 152.0–153.0 °C.

(*E*)-2-Phenyl-3-(phenylimino)-5-(pyridin-2-yl)-1,2,5-oxa-diazinan-4-one (6a). (0.36 g, 70%): yellow prisms; mp 122.5–123.5 °C (from MeOH).

(*E*)-5-(4-Methylpyridin-2-yl)-2-phenyl-3-(phenylimino)-1,2,5-oxadiazinan-4-one (6b). (0.28 g, 52%): yellow prisms; mp 141.0–143.0 °C (from MeOH).

***N*-(4-Methylpyridin-2-yl)-2-(phenylamino)-2-(phenylimino)-ethanamide (7b).** (0.17 g, 35%): light yellow needles; mp 163.5–164.5 °C (from MeOH).

***N*-Pyridin-2-yl-5*H*-dibenzo[*d*,*f*][1,3]diazepine-6-carboxamide (11a).** (0.21 g, 65%): orange needles; mp 180.0–182.0 °C.

***N*-(4-Methylpyridin-2-yl)-5*H*-dibenzo[*d*,*f*][1,3]diazepine-6-carboxamide (11b).** (0.23 g, 69%): orange needles; mp 203.0–204.0 °C.

Details of the experimental procedures, elemental analyses and spectral data were reported earlier.[5]

Single crystals of **7a** formed simultaneously, in a small amount, together with the crystallization of **6a** from a methanolic solution. Apart from X-ray experiments, they were not investigated by other analytical or spectroscopic methods.

Single crystals of **6b** suitable for X-ray diffraction were obtained from an acetonitrile solution, **7a** and **7b** from methanol, and **11a** from toluene: a hot solution of the appropriate compound was filtered, left to cool to ambient temperature and filtered again. The crystals were grown by the slow evaporation of the resulting saturated solution at room temperature.

It should be mentioned here that some of the compounds reported earlier crystallised with solvent molecules: 0.425 molecules of methanol per one molecule of **5a**[4] and 0.5 molecules of toluene per one molecule of **11b**.[8]

Crystal structure determination

Single-crystal diffraction data of the studied compounds—**6b**, **7a**, **7b**, and **11a**—were collected on a Nonius KappaCCD diffractometer using Mo-Kα radiation (λ = 0.71073 Å) selected by a graphite monochromator. The scan angle and the distance of the crystal to the detector were fixed at 1° per frame and 40 mm, respectively. The diffracted intensity was collected at a temperature of 293 K up to 27.5° of the θ angle, except of **11a**, for which there were no significant Bragg reflections above 26.0°. Data reduction, including absorption corrections by the multi-scan method, was performed using the HKL DENZO and SCALEPACK programs.[6a] All X-ray structures were solved by direct methods using the SIR92 program.[14a] Anisotropic displacement parameters were refined against F^2 for all non-hydrogen atoms using SHELX97.[14b] The H-atoms of the aromatic rings, methyl and methylene groups were found in the Fourier difference maps; they were included in the refinement following the appropriate geometrical constraints (aromatic C–H = 0.93 Å, methylene C–H = 0.97 Å and methyl C–H = 0.96 Å) and using the riding model with the isotropic displacement factors $U_{izo} = 1.2U_{eq}$ of the parent atoms. The methyl groups were disordered and described by two sites rotated by 60° with respect to one from another. H-atoms attached to N-atoms were located in the Fourier difference maps and were refined using DFIX restraints with a target value of the N–H bond length (0.88 Å), and with an assumed estimated standard deviation of 0.01 Å. Crystal data, experimental conditions and details of the refinement procedure are given in Table 1.

DFT calculations

The calculations were performed by the use of the Turbomole quantum chemical package[15a] for geometry optimisations and the Gaussian03 suite of programs[15b] for NBO and MK analyses. Density functional theory (DFT) with the B3LYP (Gaussian) functional[15c–e] and aug-cc-pVDZ[15f,g] or 6-311++(d,p) basis sets, respectively, were employed. The COSMO solvent model with default parameters for atomic radii implemented in Turbomole and dielectric constants (ε) of 2.4, 7.5 and 38.2 were used to simulate the solvent effects in toluene, THF and DMF, respectively. Atomic charges were assessed from NBO or Merz–Singh–Kolman populations.

The models for **5a** and **6a** were taken from their crystal structures.[4,5] Geometries were fully optimised *in vacuo* and then re-optimised within the COSMO model in solvents of various polarity: toluene, THF and DMF. For the deprotonated species **5′a**, derived from **5a**, the geometry optimisations were performed after proton abstraction.

In order to assess the relative stability of the putative analogue, **6′a**, of **6a** with a seven-membered ring (a conceivable reaction product for the dialkylation of **5a** with ethylene diiodide), the geometry of **6a** was re-optimized after introducing an extra –CH_2– group into the ring. The energy of the CH_2

moiety was calculated as the average of the energy differences between consecutive alkanes for the number of carbon atoms from $n = 2$ up to $n = 6$. The relative stability of the putative seven-membered ring product **6′a** was calculated as: $\Delta E = E_{\text{seven-membered ring}} - E_{\text{six-membered ring}}$ and compared with $E_{\text{methylene group}}$.

Acknowledgements

The authors thank the X-Ray Laboratory, Faculty of Chemistry, Jagiellonian University, for making the Nonius KappaCCD diffractometer available.

References

1 S. W. Bartlett, S. J. Coles, D. B. Davies, M. B. Hursthouse, H. İbioğlu, A. Kiliç, R. A. Shaw and İ. Ün, *Acta Crystallogr., Sect. B: Struct. Sci.*, 2006, **62**, 321–329.
2 (*a*) T. Y. Fu, Z. Liu, G. Olovsson, J. R. Scheffer and J. Trotter, *Acta Crystallogr., Sect. B: Struct. Sci.*, 1997, **53**, 293–299; (*b*) T. Y. Fu, J. R. Scheffer and J. Trotter, *Acta Crystallogr., Sect. B: Struct. Sci.*, 1997, **53**, 300–305; (*c*) T. Y. Fu, G. Olovsson, J. R. Scheffer and J. Trotter, *Acta Crystallogr., Sect. C: Cryst. Struct. Commun.*, 1996, **52**, 2347–2349; (*d*) T. Y. Fu, G. Olovsson, J. R. Scheffer and J. Trotter, *Tetrahedron Lett.*, 1995, **36**, 4353–4356.
3 (*a*) D. Furukawa and A. Matsumoto, *Macromolecules*, 2007, **40**, 6048–6056; (*b*) T. Hosoya, H. Uekusa, Y. Ohashi, T. Ohhara, I. Tanaka and N. Niimura, *Acta Crystallogr., Sect. B: Struct. Sci.*, 2006, **62**, 153–160.
4 M. Hodorowicz, K. Stadnicka, B. Trzewik and B. Zaleska, *Acta Crystallogr., Sect. E: Struct. Rep. Online*, 2008, **64**, o599–o600.
5 B. Trzewik, D. Cież, M. Hodorowicz and K. Stadnicka, *Synthesis*, 2008, 2977–2985.
6 (*a*) Z. Otwinowski and W. Minor, *Methods Enzymol.*, 1997, **276**, 307–326; (*b*) *COLLECT: Data Collection Software*, Nonius BV, Delft, The Netherlands, 1998.
7 L. J. Farrugia, *J. Appl. Crystallogr.*, 1997, **30**, 565.
8 M. Hodorowicz, K. Stadnicka, B. Trzewik and B. Zaleska, *Acta Crystallogr., Sect. E: Struct. Rep. Online*, 2007, **63**, o4115.
9 (*a*) The term "hydrogen-bond-like" was proposed in: H. Rostkowska, M. J. Nowak, L. Lapinski and L. Adamowicz, *Phys. Chem. Chem. Phys.*, 2001, **3**, 3012–3017; (*b*) F. H. Allen, O. Kennard, D. G. Watson, L. Brammer, A. G. Orpen and R. Taylor, in *International Tables for Crystallography, vol. C: Mathematical, Physical and Chemical Tables*, ed. A. J. C. Wilson, Kluwer Academic Publishers, Dordrecht, 1995, pp. 685–706; (*c*) *Cambridge Structural Database, v. 5.30*, 2008; F. H. Allen, *Acta Crystallogr., Sect. B: Struct. Sci.*, 2002, **58**, 380–388; (*d*) V. L. Rusinov, T. V. Dragunova, V. A. Zyryanov, G. G. Aleksandrov and O. N. Chupakhin, *Khim. Geterotsikl. Soedin.*, 1986, 1668.
10 (*a*) A. E. Reed, L. A. Curtiss and F. Weinhold, *Chem. Rev.*, 1988, **88**, 899–926; (*b*) B. H. Besler, K. M. Merz and P. A. Kollman, *J. Comput. Chem.*, 1990, **11**, 431–439; (*c*) U. C. Singh and P. A. Kollman, *J. Comput. Chem.*, 1984, **5**, 129–145.
11 A. G. Giumanini, N. Toniutti, G. Verardo and M. Merli, *Eur. J. Org. Chem.*, 1999, 141–144.
12 (*a*) D. Geffken, H. Zydowitz and A. Ploetz, *Z. Naturforsch., B: Chem. Sci.*, 2005, **60**, 967–972; (*b*) Y. Kamitori, *Heterocycles*, 2000, **53**, 107–113; (*c*) V. Gouverneur and L. Ghosez, *Tetrahedron*, 1996, **52**, 7585–7598 and references cited therein; (*d*) M. B. Gravestock, D. W. Knight, K. M. A. Malik and S. R. Thornton, *J. Chem. Soc., Perkin Trans. 1*, 2000, 3292–3305 and references cited therein; (*e*) M. B. Gravestock, D. W. Knight and S. R. Thornton, *J. Chem. Soc., Chem. Commun.*, 1993, 169–171; (*f*) S. Nakanishi, J. Nantaku and Y. Otsuji, *Chem. Lett.*, 1983, 341–342.
13 (*a*) M. Boruah, D. Konwar and D. Dutta, *Indian J. Chem., Sect. B: Org. Chem. Incl. Med. Chem.*, 2003, **42**, 2112–2114; (*b*) A. Freisleben, P. Schieberle and M. Rychlik, *J. Agric. Food Chem.*, 2002, **50**, 4760–4768; (*c*) P. S. Branco, S. Prabhakar, A. M. Lobo and D. J. Williams, *Tetrahedron*, 1992, **48**, 6335–6360; (*d*) K. G. B. Torsell, in *Nitrile Oxides, Nitrones, and Nitronates in Organic Synthesis: Novel Strategies in Synthesis*, ed. H. Feuer, VCH Publishers, Weinheim, 1988, ch. 3, pp. 75–93.
14 (*a*) A. Altomare, M. C. Burla, M. Camalli, G. Cascarano, C. Giacovazzo, A. Guagliardi and G. Polidori, *J. Appl. Crystallogr.*, 1994, **27**, 435; (*b*) G. M. Sheldrick, *Acta Crystallogr., Sect. A: Found. Crystallogr.*, 2008, **64**, 112–122.
15 (*a*) *Turbomole v. 6.0*, Turbomole GmbH, Karlsruhe Germany, 2009 (available from http://www.turbomole.com); (*b*) M. J. Frisch, G. W. Trucks, H. B. Schlegel, G. E. Scuseria, M. A. Robb, J. R. Cheeseman, J. A. Montgomery, Jr., T. Vreven, K. N. Kudin, J. C. Burant, J. M. Millam, S. S. Iyengar, J. Tomasi, V. Barone, B. Mennucci, M. Cossi, G. Scalmani, N. Rega, G. A. Petersson, H. Nakatsuji, M. Hada, M. Ehara, K. Toyota, R. Fukuda, J. Hasegawa, M. Ishida, T. Nakajima, Y. Honda, O. Kitao, H. Nakai, M. Klene, X. Li, J. E. Knox, H. P. Hratchian, J. B. Cross, V. Bakken, C. Adamo, J. Jaramillo, R. Gomperts, R. E. Stratmann, O. Yazyev, A. J. Austin, R. Cammi, C. Pomelli, J. Ochterski, P. Y. Ayala, K. Morokuma, G. A. Voth, P. Salvador, J. J. Dannenberg, V. G. Zakrzewski, S. Dapprich, A. D. Daniels, M. C. Strain, O. Farkas, D. K. Malick, A. D. Rabuck, K. Raghavachari, J. B. Foresman, J. V. Ortiz, Q. Cui, A. G. Baboul, S. Clifford, J. Cioslowski, B. B. Stefanov, G. Liu, A. Liashenko, P. Piskorz, I. Komaromi, R. L. Martin, D. J. Fox, T. Keith, M. A. Al-Laham, C. Y. Peng, A. Nanayakkara, M. Challacombe, P. M. W. Gill, B. G. Johnson, W. Chen, M. W. Wong, C. Gonzalez and J. A. Pople, *GAUSSIAN 03 (Revision B.02)*, Gaussian, Inc., Wallingford, CT, 2004; (*c*) A. D. Becke, *Phys. Rev. A: At., Mol., Opt. Phys.*, 1988, **38**, 3098–3100; (*d*) A. D. Becke, *J. Chem. Phys.*, 1993, **98**, 5648–5652; (*e*) J. P. Perdew, *Phys. Rev. B: Condens. Matter*, 1986, **33**, 8822–8824; (*f*) D. Feller, *J. Comput. Chem.*, 1996, **17**, 1571–1586; (*g*) K. L. Schuchardt, B. T. Didier, T. Elsethagen, L. Sun, V. Gurumoorthi, J. Chase, J. Li and T. L. Windus, *J. Chem. Inf. Model.*, 2007, **47**, 1045–1052.

